

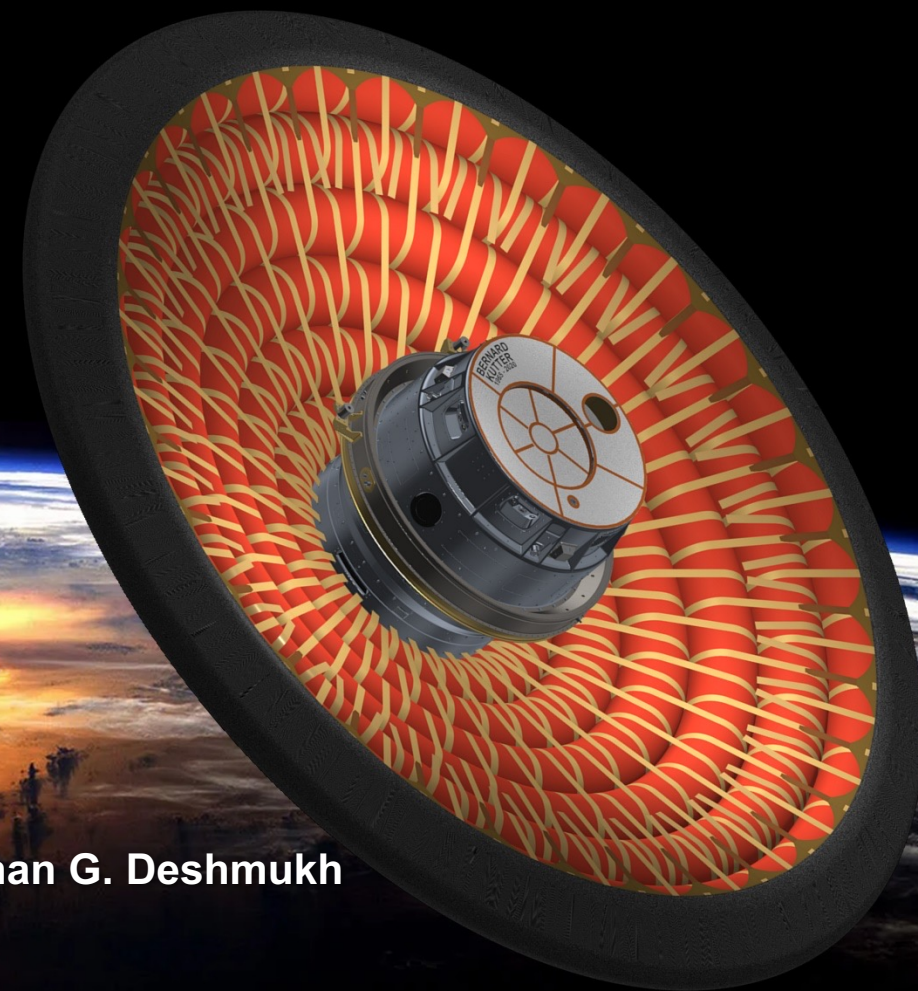


Low-Earth Orbit Flight Test
of an Inflatable Decelerator

National Aeronautics and
Space Administration



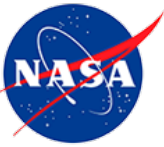
Aerodynamic Performance of the Low-Earth Orbit Flight Test of an Inflatable Decelerator (LOFTID) Technology Demonstration Mission



Ashley M. Korzun, Brian R. Hollis, Adam J. Wise, Derek S. Liechty, Rohan G. Deshmukh
NASA Langley Research Center

Christopher D. Karlgaard
Analytical Mechanics Associates – NASA Langley Research Center

AIAA SciTech Forum
8-12 January 2024



Introduction

LOFTID: Low-Earth Orbit Flight Test of an Inflatable Decelerator

- **November 10, 2022: launch from Vandenberg Space Force Base and splashdown in the Pacific Ocean off the coast of Hawaii**
- **Largest blunt-body flown to date**
- **Successful demonstration of inflatable aeroshell technology at scale and conditions relevant to Earth and Mars EDL**

Key requirements relevant to aerodynamics:

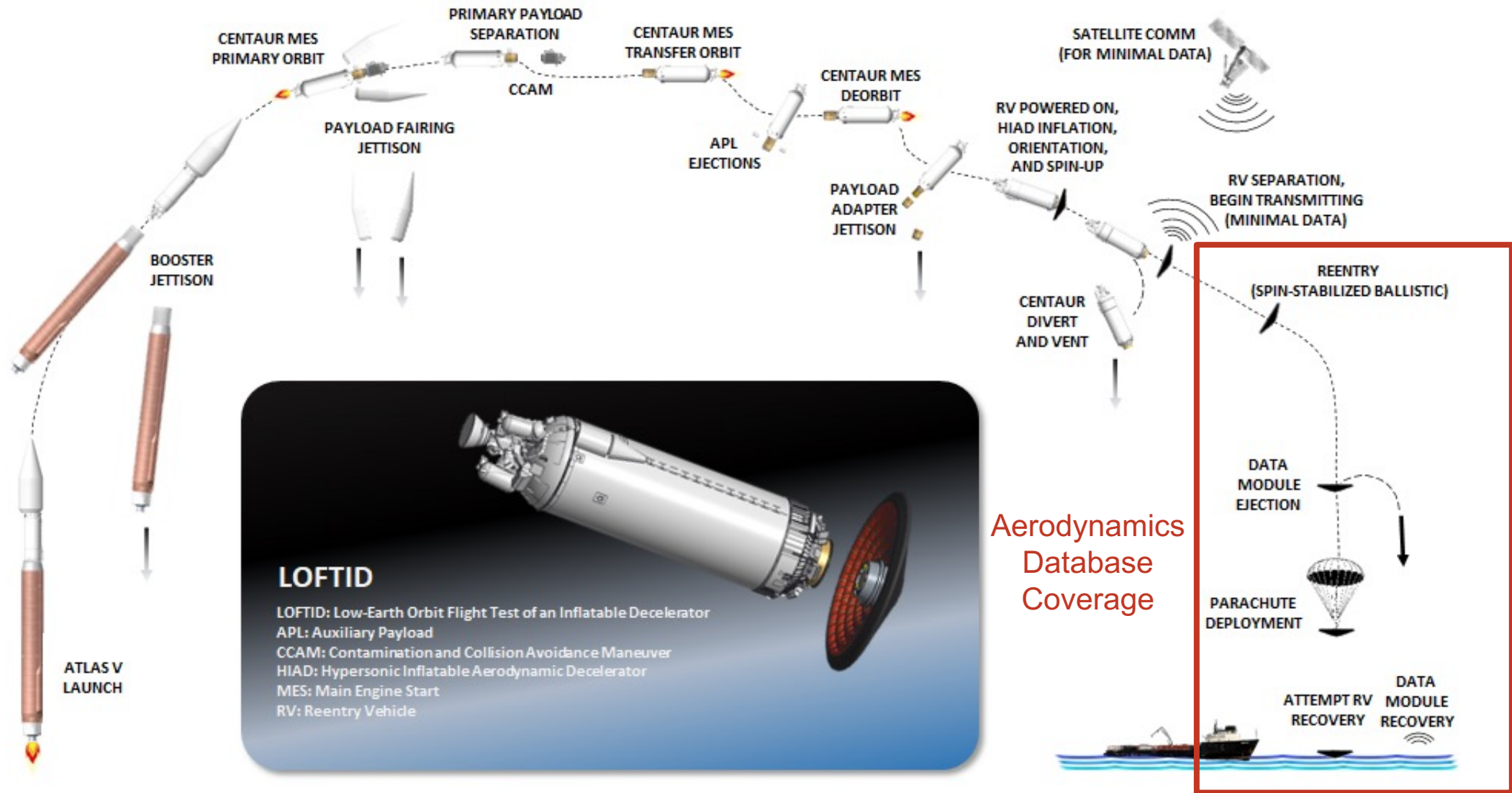
- **Maintain total angle of attack less than 20° from hypersonic through subsonic regimes to Mach 0.7**
- **Demonstrate performance as a decelerator equivalent to a 70° sphere-cone rigid aeroshell**



Image credit: NASA



LOFTID Concept of Operations





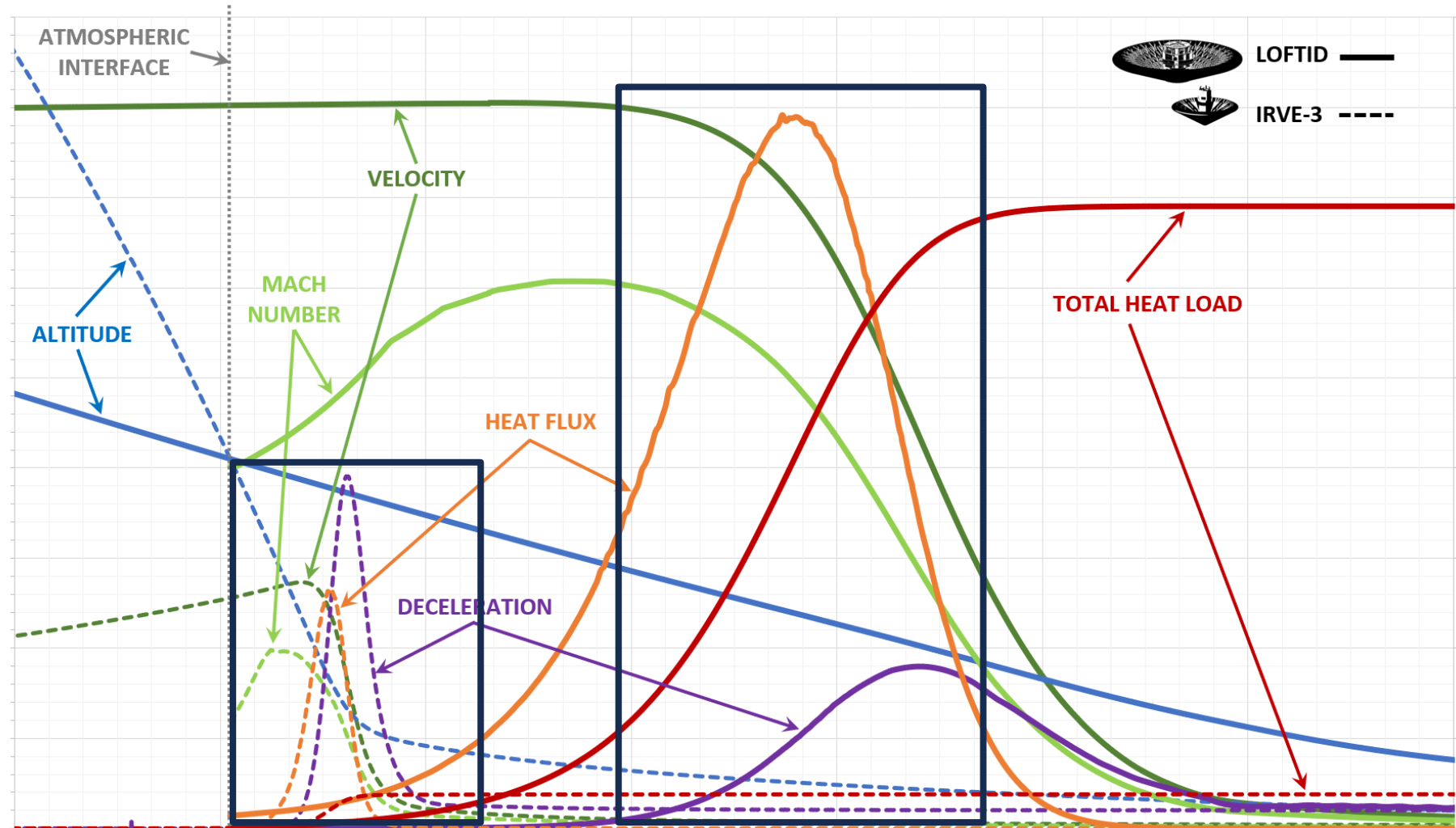
From IRVE-3 to LOFTID

IRVE-3: Inflatable Re-entry Vehicle Experiment-3

- HIAD flight demo (2012)
- Suborbital sounding rocket flight
- 3m diameter aeroshell
- 60° sphere-cone

LOFTID

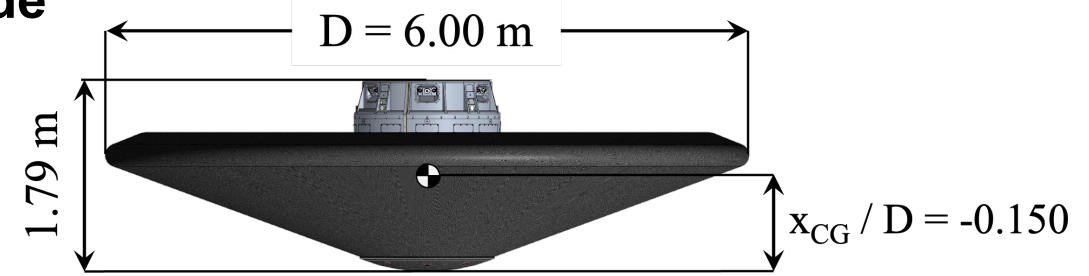
- Nearly 3x the entry velocity
- Orbital re-entry flight
- 6m diameter aeroshell
- 70° sphere-cone



Aerodynamics Database Overview

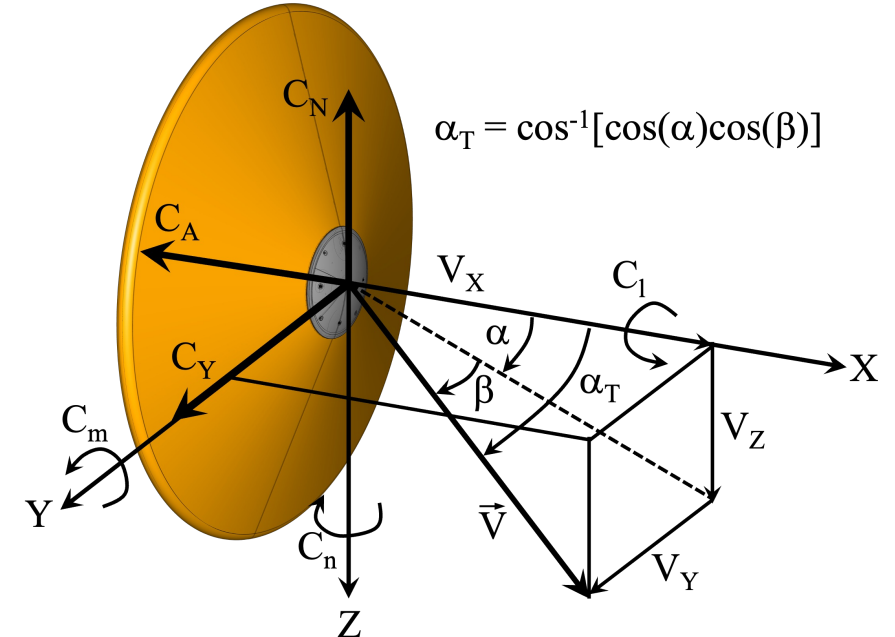
➤ **Aerodynamics database provides 6-DOF coefficients as a function of flight conditions and vehicle attitude**

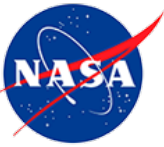
- Non-continuum and continuum flight regimes
- Static aerodynamics and dynamic damping
- Uncertainties provided as function of flight regime and reflect underlying methods and data sources



➤ **Aerodynamics datasets, methods, tools, and implementation draw on flight experience from IRVE-II and IRVE-3, as well as prior HIAD design studies and rigid aeroshell missions**

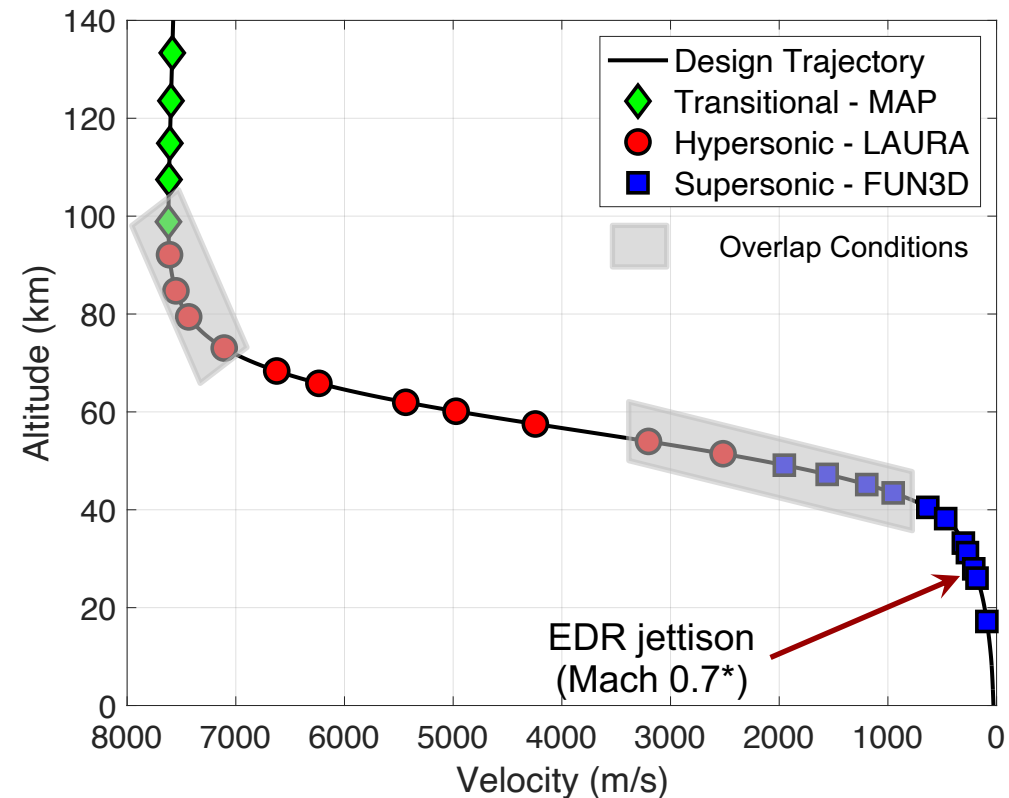
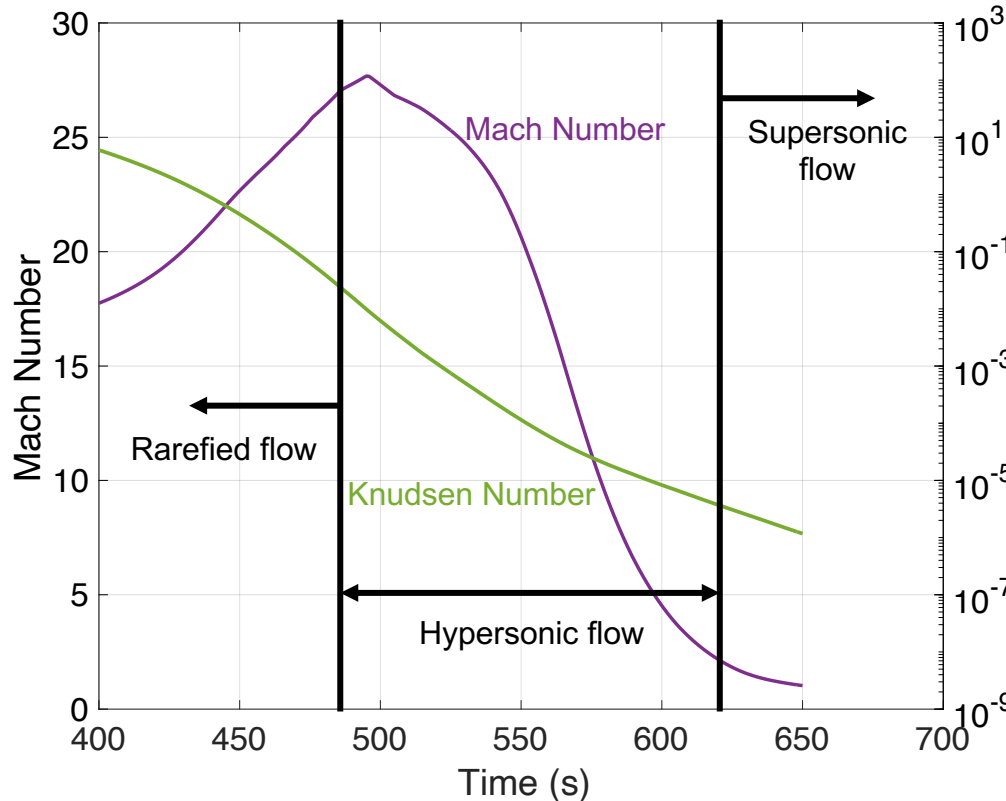
➤ **Vehicle modeled as axisymmetric, smooth, and rigid**





Design Reference Trajectory

- Discrete points along a design reference trajectory used to define conditions for computational fluid dynamics (CFD) data generation
- Overlaps between flow regimes blend data from different sources



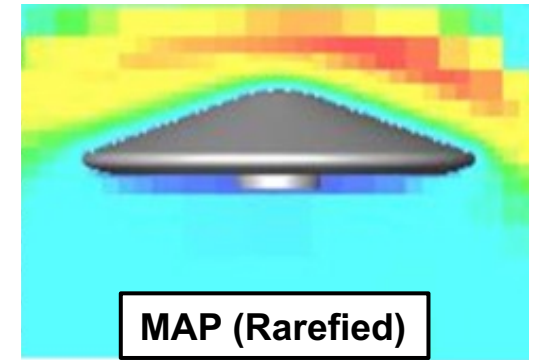
*Nominal target

*See paper by Deshmukh et al. in this session for more detail

Static Aerodynamics

	Flight Regime	Range	Input Parameters	Source
Non-Continuum	Free-Molecular	$Kn > 3.018, 0^\circ \leq \alpha_T \leq 180^\circ$	α_T	DAC [12]
	Transitional	$0.00572 \leq Kn \leq 3.018, 0^\circ \leq \alpha_T \leq 8^\circ$	α_T, Kn	MAP [13]
Continuum	Hypersonic	$M_\infty \geq 7.88$ and $Kn < 0.00572, 0^\circ \leq \alpha_T \leq 8^\circ$	α_T, M_∞	LAURA [14]
	Supersonic	$0.89 < M_\infty \leq 6.10, 0^\circ \leq \alpha_T \leq 20^\circ$	α_T, M_∞	FUN3D [15]
	Mid-Subsonic	$0.30 < M_\infty \leq 0.89, 0^\circ \leq \alpha_T \leq 40^\circ$	α_T, M_∞	FUN3D
	Low-Subsonic	$M_\infty \leq 0.30, 0^\circ \leq \alpha_T \leq 40^\circ$	α_T	FUN3D

- Relevant methods and tools dictated by flow regime
- Aerodynamics data tabulated as functions of α_T and Kn or M_∞
- Forebody-only solutions used for hypersonic conditions and above
- Full-geometry solutions used for supersonic conditions and below
- Continuum datasets linearly blended between breakpoints

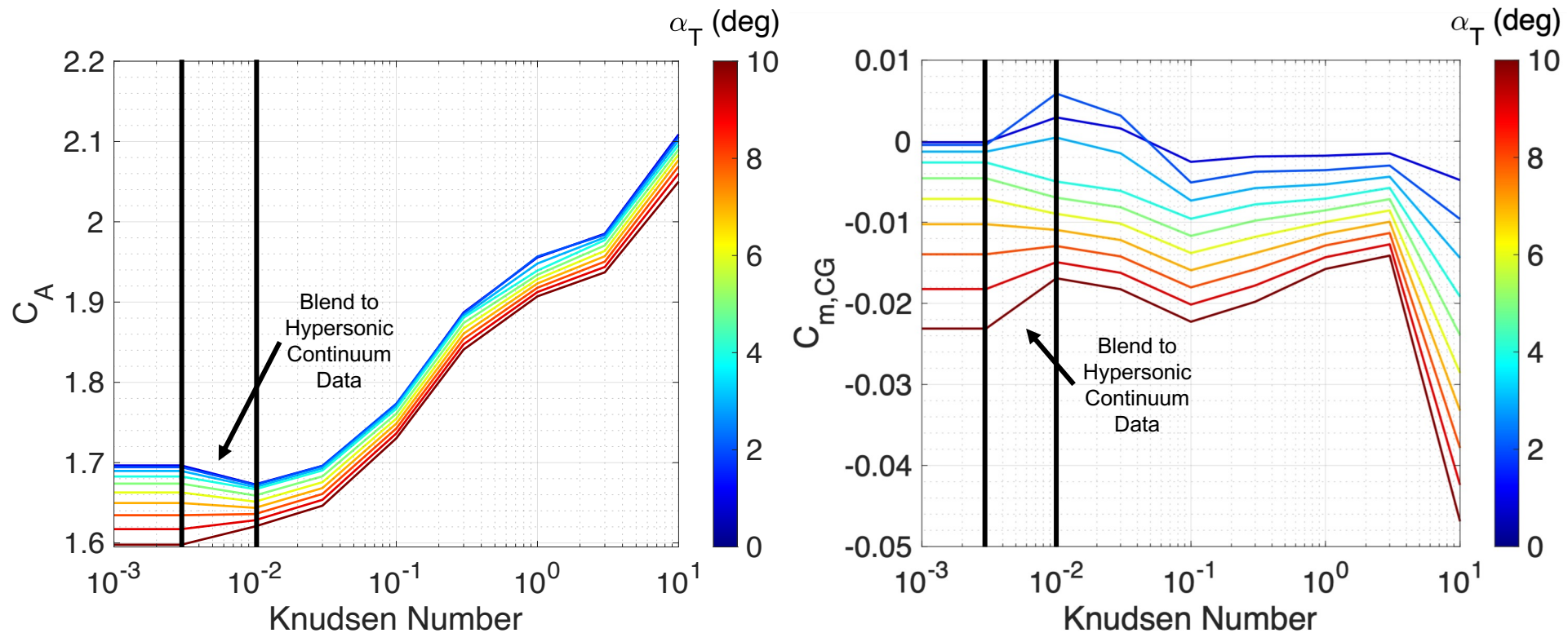


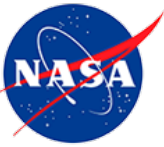
*See paper by Hollis et al. in this session for more detail



Static Aerodynamics Database – Non-Continuum

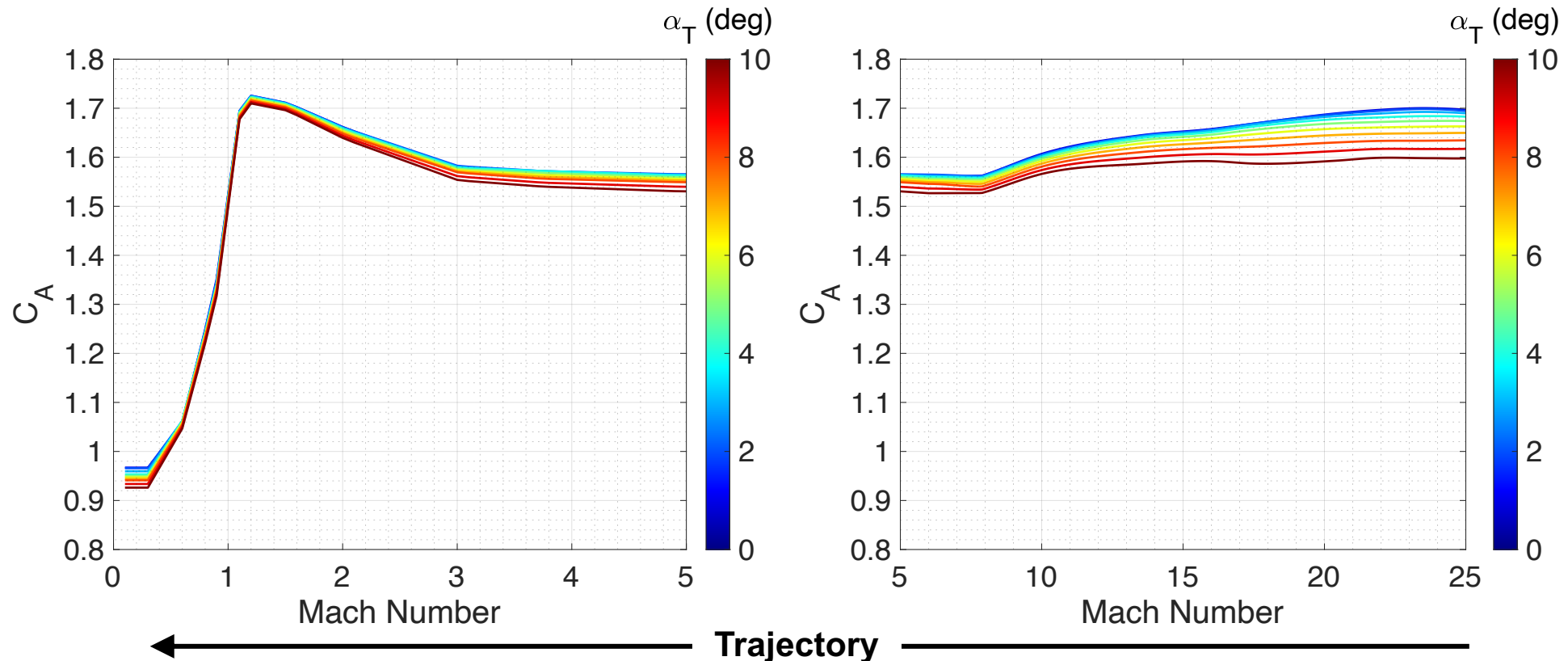
- Non-continuum aerodynamics generated using the MAP DSMC code
- Replaces traditional sine-squared bridging function through transitional flow regime
- Altitude range: above 98 km
- Minor static instability at low α_T ($< 2^\circ$) for $0.003 < Kn < 0.1$





Static Aerodynamics Database – Continuum

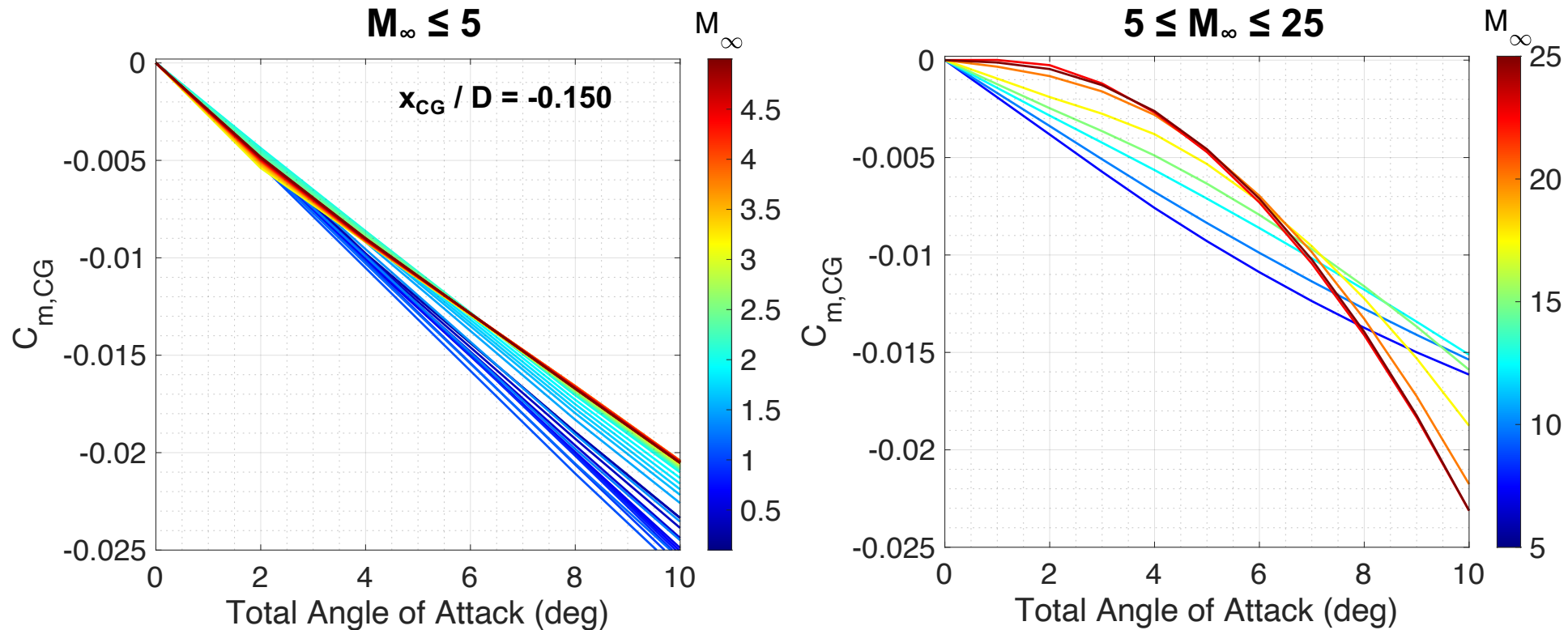
- Entire dataset for continuum conditions generated using CFD
- C_A trend with both M_∞ and α_T are as-expected for a 70° sphere-cone at Earth
- Sensitivity of C_A to α_T decreases along the re-entry trajectory
- Full vehicle geometry used for all static coefficients below Mach 6.10





Static Aerodynamics Database – Continuum

- **Statically stable across the full continuum regime**
- **High hypersonic conditions show increasing static stability at very low α_T from non-continuum conditions**

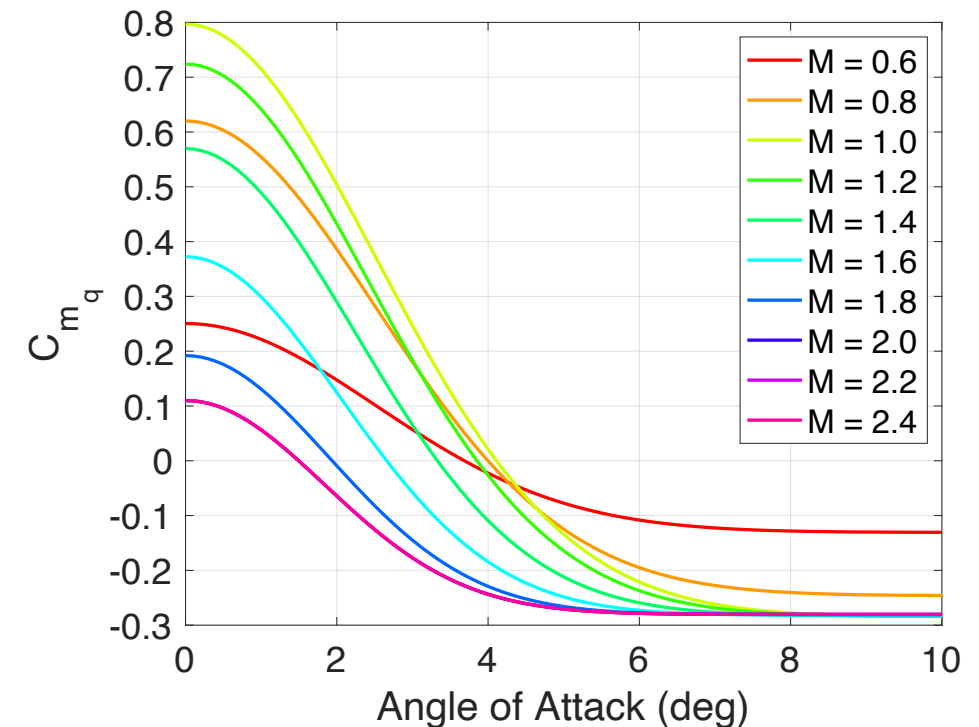




Pitch Damping Database

	Flight Regime	Range	Input Parameters	Source
Non-Continuum	Free-Molecular	$Kn \geq 10.0, 0^\circ \leq \alpha_T \leq 180^\circ$	none	-
	Transitional	$0.001 < Kn < 10.0, 0^\circ < \alpha_T < 40^\circ$	α_T, Kn	-
Continuum	Hypersonic	$M_\infty \geq 6.0$ and $Kn < 0.001, 0^\circ \leq \alpha_T \leq 40^\circ$	α_T, M_∞	IRVE-3
	Supersonic	$0.65 \leq M_\infty < 3.0, 0^\circ \leq \alpha_T \leq 40^\circ$	α_T, M_∞	IRVE-3
	Subsonic	$M_\infty < 0.65, 0^\circ \leq \alpha_T \leq 40^\circ$	α_T, M_∞	IRVE-3

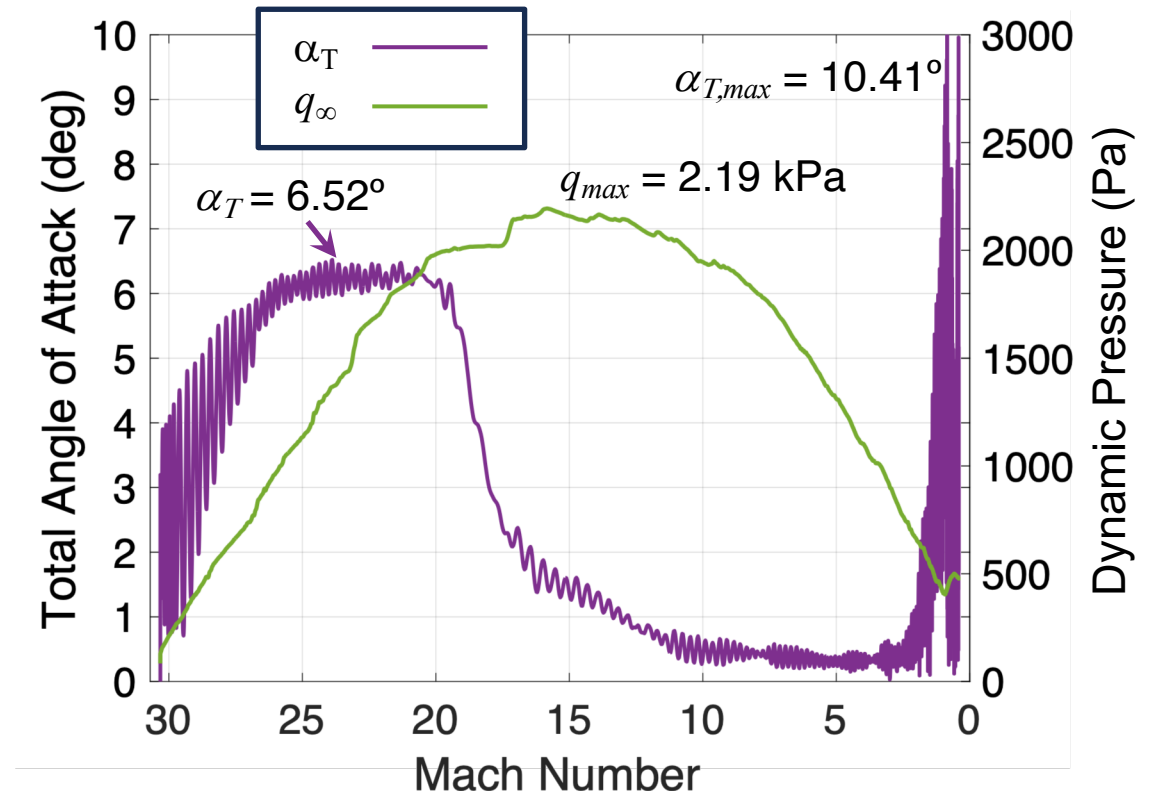
- **Blunt bodies are characteristically dynamically unstable at low supersonic to transonic conditions**
- **Free-molecular: $C_{mq} = -0.32$ (constant)**
- **Transitional: sine-squared blend between free-molecular and hypersonic values as a function of Kn**
- **Hypersonic: $C_{mq} = -0.20$ (constant)**
- **IRVE-3 ballistic range functional forms for $0.65 \leq M_\infty \leq 3.0$**
- **C_{mq} constant for $M_\infty \leq 0.65$**





Reconstructed As-Flown Performance

- IMU data were not captured by the data recorder, preventing reconstruction of the as-flown aerodynamics
- Atmosphere-relative trajectory and attitude reconstructed using FADS and on-board video data*
- Shift in α_T :
 - Aeroshell settling into the nominal drag position from its zero-g inflation position
 - Aligns with a density change in the local atmosphere and resulting "bump" in dynamic pressure

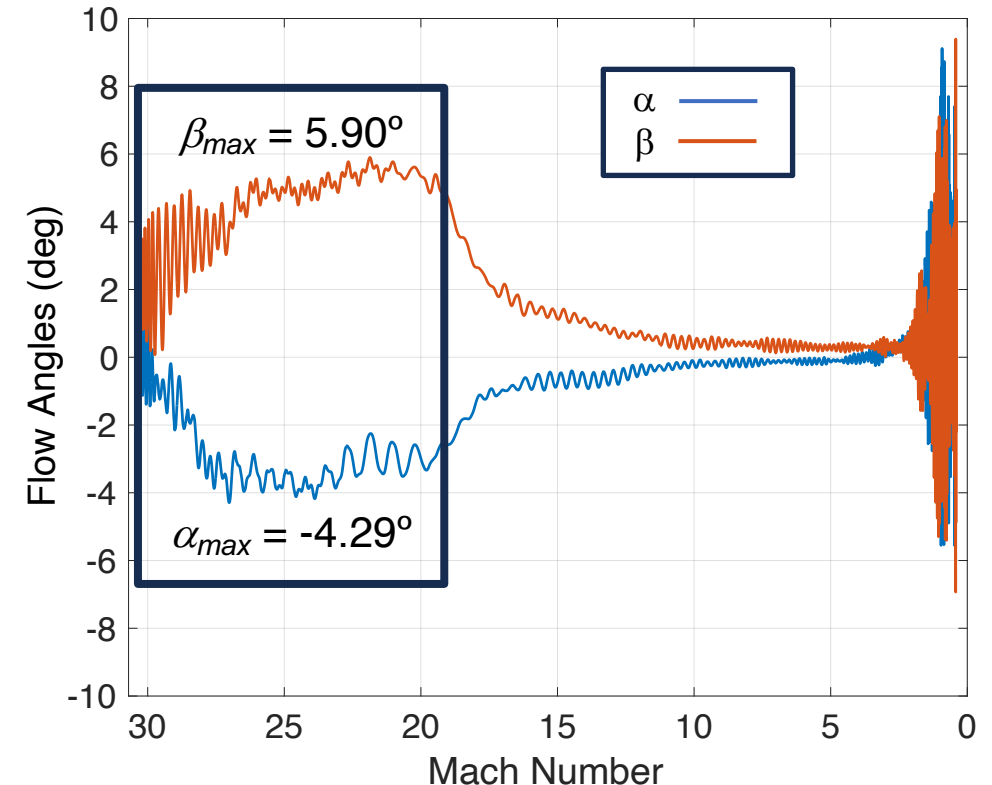


*See paper by Karlgaard et al. in this session for more detail



Reconstructed As-Flown Performance

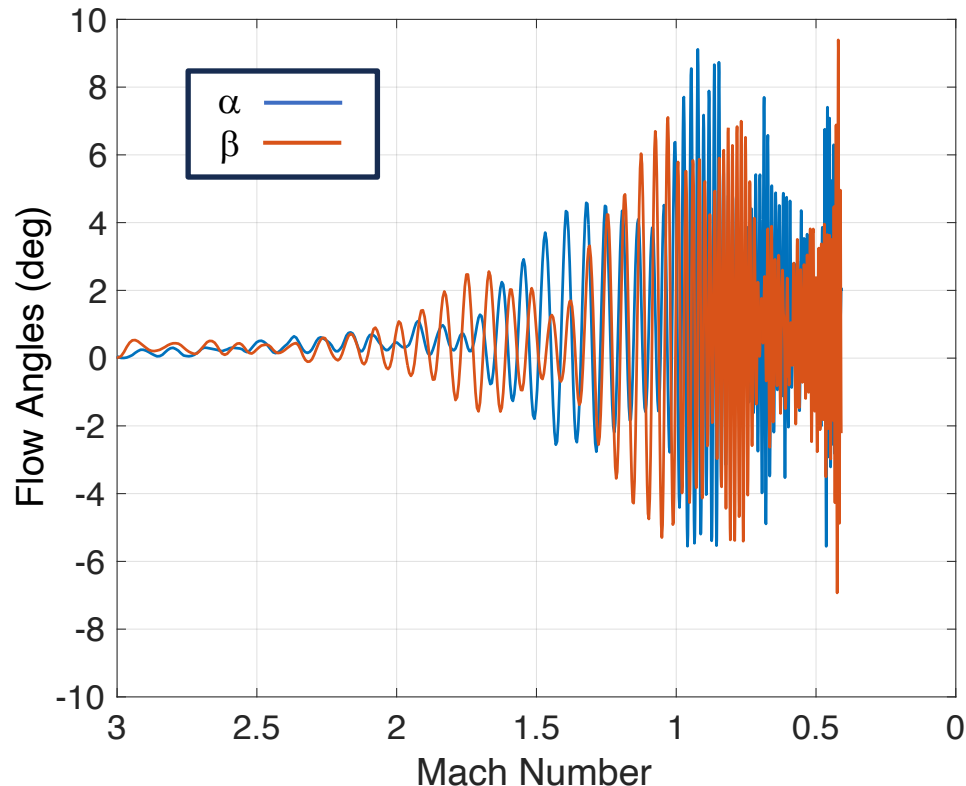
- Aeroshell orientation relative to the rigid nose was sufficient off-center to trim hypersonically before settling into the nominal drag position
- As expected, attitude begins to increase with deceleration through supersonic to subsonic conditions due to inherent dynamic instability of the blunt-body shape
- On-board video data confirmed no attitude or attitude rate excursions
- Nominal spin rate: 18 deg/s; Reconstructed estimated spin rate: 17.7 deg/s



*See papers by Deshmukh et al. and Karlgaard et al. in this session for more detail

Reconstructed As-Flown Performance

- Peak attitude well below the 20° mission requirement ($\alpha_{T,max} = 10.41^\circ$)
- Vehicle observed from the recovery vessel to be highly stable under parachute
- Both the data recorder and vehicle were successfully recovered from the ocean



$$\alpha_{max} = 9.12^\circ$$

$$\beta_{max} = 9.39^\circ$$



Image credit: NASA

- Splashdown was 5.53 nmi from target, with the vehicle visible from the recovery vessel while descending under parachute



Summary

- **LOFTID mission requirements were successfully met through orbital re-entry of a 6m diameter inflatable aeroshell**
- **Peak total angle of attack remained well below the 20° requirement**
- **Aerodynamics database for LOFTID leveraged and expanded on prior suborbital flight experience, with demonstration of decelerator performance and stability**
- **Lack of IMU data limited reconstruction of vehicle performance without reliance on nominal pre-flight aerodynamics**



Image credit: Greg Swanson (NASA)



Back-up



Aerodynamics Uncertainties

- Dispersed aerodynamics applied through Monte Carlo flight mechanics analysis to establish vehicle performance and to verify requirements pre-flight
- Uncertainties based on flight experience from Genesis, IRVE, and IRVE-3
- Adders and multipliers used to independently disperse trim attitude (intercept) and static stability (slope), respectively

Static Aerodynamics (Uncorrelated)

Flight Regime	C_A	C_N, C_Y	C_m, C_n	C_l
Free-Molecular / Transitional $Kn > 0.1$	$\pm 5\%$	$\pm 0.01, \pm 20\%$	$\pm 0.005, \pm 20\%$	$\pm 1.24 \times 10^{-6}$
Hypersonic $M_\infty < 10$	$\pm 3\%$	$\pm 0.01, \pm 20\%$	$\pm 0.003, \pm 20\%$	$\pm 1.24 \times 10^{-6}$
Supersonic $1.5 < M_\infty < 5$	$\pm 10\%$	$\pm 0.01, \pm 20\%$	$\pm 0.005, \pm 20\%$	$\pm 1.24 \times 10^{-6}$
Transonic $0.4 < M_\infty < 1.5$	$\pm 10\%$	$1.25 \times \text{Supersonic}$	$1.25 \times \text{Supersonic}$	$\pm 1.24 \times 10^{-6}$

Dynamic Damping (Correlate)

Flight Regime	C_{m_q}	C_{n_r}
Transitional / Free-Molecular $Kn > 0.1$	± 0.15	± 0.15
Hypersonic $M_\infty > 6$	± 0.15	± 0.15
Supersonic $1.5 < M_\infty < 3$	$+0.4 \times [1.5, 0.5] - 0.4 + [0.1, 0.0]$	$+0.4 \times [1.5, 0.5] - 0.4 + [0.1, 0.0]$
Transonic $1 < M_\infty < 1.5$	$1.25 \times \text{Supersonic}$	$1.25 \times \text{Supersonic}$

- All moments dispersed about the CG
- Fixed shift applied to dynamic damping forces more cases to be less stable

$$C_{disp} = [C_{nominal}(\alpha, \beta) + U_C^A](1 + U_C^M)$$

$$C_{m_q,disp} = (C_{m_q,nominal}(\alpha, \beta) - 0.4) * U_C^M + 0.4 + U_C^A$$